Molecular Therapy
Nucleic Acids
Original Article

# Single-cell analysis of the survival mechanisms of fratricidal CAR-T targeting of T cell malignancies

Hui Hu,[1,2,7] Ling Tang,[3,7] Yuyan Zhao,[4] Jiali Cheng,[5] Mei Huang,[5] Yong You,[6] Ping Zou,[6] Qian Lei,[1] Xiaojian Zhu,[5] and An-Yuan Guo[1,4]

[1]Department of Hematology, West China Biomedical Big Data Center, West China Hospital, Med-X Center for Informatics, Sichuan University, Chengdu 610041, China; [2]Department of Laboratory Medicine, Tongji Hospital, Tongji Medical College, Huazhong University of Science and Technology, Wuhan, Hubei 430030, China; [3]Department of Hematology, Renmin Hospital of Wuhan University, Wuhan 430060, China; [4]Hubei Bioinformatics & Molecular Imaging Key Laboratory, College of Life Science and Technology, Huazhong University of Science and Technology, Wuhan, Hubei 430074, China; [5]Department of Hematology, Tongji Hospital, Tongji Medical College, Huazhong University of Science and Technology, Wuhan 430030, China; [6]Institute of Hematology, Union Hospital, Tongji Medical College, Huazhong University of Science and Technology, Wuhan 430022, China

**Chimeric antigen receptor T (CAR-T) cell therapy targeting T cell tumors still faces many challenges, one of which is its fratricide due to the target gene expressed on CAR-T cells. Despite this, these CAR-T cells can be expanded *in vitro* by extending the culture time and effectively eliminating malignant T cells. However, the mechanisms underlying CAR-T cell survival in cell subpopulations, the molecules involved, and their regulation are still unknown. We performed single-cell transcriptome profiling to investigate the fratricidal CAR-T products (CD26 CAR-Ts and CD44v6 CAR-Ts) targeting T cells, taking CD19 CAR-Ts targeting B cells from the same donor as a control. Compared with CD19 CAR-Ts, fratricidal CAR-T cells exhibit no unique cell subpopulation, but have more exhausted T cells, fewer cytotoxic T cells, and more T cell receptor (TCR) clonal amplification. Furthermore, we observed that fratricidal CAR-T cell survival was accompanied by target gene expression. Gene expression results suggest that fratricidal CAR-T cells may downregulate their human leukocyte antigen (HLA) molecules to evade T cell recognition. Single-cell regulatory network analysis and suppression experiments revealed that exhaustion mediated by critical regulatory factors may contribute to fratricidal CAR-T cell survival. Together, these data provide valuable and first-time insights into the survival of fratricidal CAR-T cells.**

## INTRODUCTION

Chimeric antigen receptor T (CAR-T) cells are genetically modified T cells expressing a recombinant cell-surface receptor to target and kill cells expressing specific tumor-associated antigens.[1,2] CAR-T therapy has led to impressive responses and encouraging outcomes in patients with hematological malignancies. For example, CD19 CAR-T cells have shown excellent efficacy in B cell tumors, achieving remission rates of more than 90%.[3,4] In addition, Abecma is the latest CAR-T product approved by the Food and Drug Administration (FDA) for the treatment of multiple myeloma.[5] Numerous CAR-T studies have also focused on clinical trials in solid tumors.[6] However, T cell tumors still have great challenges for CAR-T therapy, one of which is the shared expression of target antigens on both parental T cells and malignant T cells, which will lead to CAR-T cell fratricide and severe immunodeficiency.[7,8]

CD4, CD5, CD7, CD30, CD70, CD26, and CD44 isoform variant 6 (CD44v6) were investigated as targets for CAR-T therapy of T cell malignancies.[7] Data from phase I clinical trials of donor-derived CD7 CAR-Ts for T cell acute lymphoblastic leukemia (T-ALL) showed complete remission (CR) rates of up to 90%. Although the continuous stimulation of T cells by CD3/CD28 antibodies is a critical factor, the mechanisms of fratricide resistance and continuing function are unclear.[9] The fratricide of CAR-T cells can be reduced by knocking out their corresponding targets in T cells, but the cytotoxicity is also reduced and their overall responsiveness is limited.[10,11] Therefore, it is extremely important to explore the suitable construction modes of CAR-T targeting of T cell tumors and to find the mechanism of their survival for the development and application of CAR-T targeting of T cell tumors.

Received 17 November 2023; accepted 16 May 2024;
https://doi.org/10.1016/j.omtn.2024.102225.

[7]These authors contributed equally

**Correspondence:** Qian Lei, Department of Hematology, West China Biomedical Big Data Center, West China Hospital, Med-X Center for Informatics, Sichuan University, Chengdu 610041, China.
**E-mail:** leiqianqian@wchscu.edu.cn
**Correspondence:** Xiaojian Zhu, Department of Hematology, Tongji Hospital, Tongji Medical College, Huazhong University of Science and Technology, No. 1095 Jiefang Road, Wuhan 430030, China.
**E-mail:** zhuxiaojian@hust.edu.cn
**Correspondence:** An-Yuan Guo, Department of Hematology, West China Biomedical Big Data Center, West China Hospital, Med-X Center for Informatics, Sichuan University, Chengdu 610041, China.
**E-mail:** guoanyuan@wchscu.edu.cn

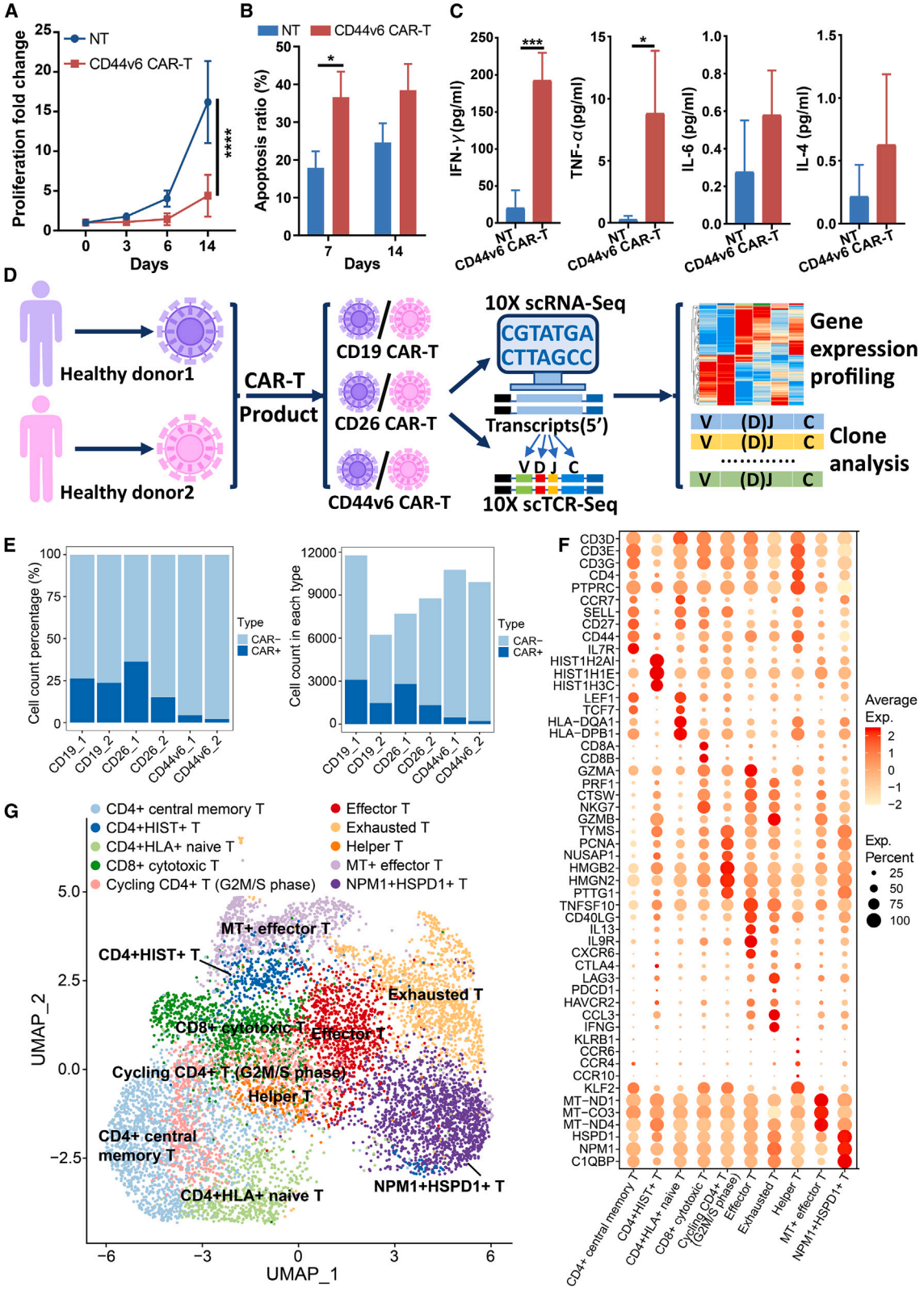


*(legend on next page)*

In recent years, CD26, CD44v6, and CD70 CAR-T cells that target T cell tumors have been reported. CD26 is overexpressed in a variety of malignancies, such as aggressive T cell lymphoma/leukemia, colon cancer, and kidney cancer,[12,13] and therefore, CD26 is a therapeutic target for a variety of tumors. CD44v6 is highly expressed in a variety of tumor cells, including T-ALL, Hodgkin's lymphoma, and thyroid cancer, but not in normal hematopoietic stem cells (HSCs). CD44v6 has been associated with poor prognosis.[14] These findings suggest that CD44v6 is an ideal target for CAR-T therapy. CD70, a ligand for CD27, is overexpressed in gliomas, renal cell carcinomas, and acute myeloid leukemia (AML), but not in normal HSCs.[15,16] CD70, CD26, and CD44v6 are expressed on T cells, leading to significant fratricide during CAR-T cell construction.[17–20] Studies demonstrated that, although there was fratricide in CD70 CAR-T, CD26 CAR-T, and CD44v6 CAR-T cells, they could be expanded *in vitro* by extended culture, effectively eliminating tumor cells and significantly inhibiting disease progression in xenograft mouse models.[17,19,20] However, how do these fratricidal CAR-T cells survive without target knockdown during the construction process?

To uncover why fratricidal CAR-Ts survived without knocking down target genes, we constructed CD19, CD26, and CD44v6 CAR-T cells from $CD3^+$ T cells from two healthy donors, where CD26 and CD44v6 CAR-T cells were fratricidal, while CD19 CAR-T cells served as controls due to the absence of fratricide. Next, single-cell RNA sequencing (scRNA-seq) coupled with single-cell T cell receptor sequencing (scTCR-seq) was conducted on these three CAR-T cells to analyze differences in cellular components, clonal amplification, gene expression, and regulation between fratricidal CAR-T and CD19 CAR-T cells. These analyses informed our understanding of the primary mechanisms of fratricidal CAR-T cell survival, which would greatly improve the research and application of CAR-T cell therapy for T cell malignancies.

## RESULTS

### Cell subpopulations in fratricidal CAR-Ts (CD26 and CD44v6) and CD19 CAR-T cells by scRNA-seq

We transduced cells with CD19/CD26/CD44v6 CAR lentivirus to construct CAR-Ts from two healthy donors as replicates. T cells transfected with CD44v6 CAR lentivirus exhibited slow proliferation (Figure 1A), increased apoptosis (Figure 1B), and increased cytokine secretion without external antigen stimulation (Figure 1C). Findings were similar in CD26 CAR-Ts.[18] To better understand the immune state of CAR-T cells, we performed scRNA-seq and scTCR-seq for further analysis (Figure 1D). After rigorous quality control (QC) and filtering, we obtained 9,074–13,530 cells per sample (Table S1). Next, we focused on T cells expressing CAR as CAR-positive ($CAR^+$) cells.[21] The percentage of $CAR^+$ cells in these samples ranged from 2.11% to 36.92% (a total of 9,365 $CAR^+$ cells for all six samples, Table S2; Figure 1E). Notably, CAR gene expression in fratricidal CAR-Ts was significantly lower than that in CD19 CAR-Ts (Figure S1A). Since the cell-cycle phase affected the clustering results, we removed the effect with cell-cycle scores by regression (Figures S1B and S1C).

After dimensionality reduction with uniform manifold approximation and projection (UMAP), $CAR^+$ cells were clustered into 10 subpopulations, which were annotated based on cluster-specific highly expressed genes and well-known T cell marker genes (Figures 1F, 1G, S1D–S1F, and S2). For example, a cluster with cells specifically overexpressing LAG3, PDCD1, and HAVCR2 was annotated as an exhausted T cell cluster, while cells specifically overexpressing TCF7, LEF1, human leukocyte antigen (HLA)-DPB1, and HLA-DRA were classified as $CD4^+HLA^+$ naive T cells. In addition, the $MT^+$ effector T subpopulation was characterized by highly expressed mitochondrial genes like MT-ND1 and MT-CO3 and the effector genes GZMB, CTSW, and NKG7, suggesting that $MT^+$ effector T cells are critical components of $CAR^+$ cells. Similarly, cells without CAR expression were defined as CAR-nonexpressing ($CAR^-$) cells, which were clustered into 12 subpopulations (Figure S3A). Multilymphoid progenitor cells and $CD4^+$ T cell subpopulations were added, compared with $CAR^+$ cells (Figures S3B–S3D). In aggregate, we clearly defined the composition of cell subpopulations in CD19, CD26, and CD44v6 CAR-Ts.

### Survival of fratricidal CAR-T cells accompanied by target gene expression

As a relatively high percentage of T cells expressed CD26 and CD44v6 (Figures 2A and S4A), we analyzed the expression levels of CD26 and CD44 in CAR-Ts to investigate whether the fratricidal CAR-Ts survived the effect of the CAR-T target gene. T cells expressing CD26 or CD44 were defined as $CD26^+$ cells or $CD44^+$ cells. CD26 or CD44 was expressed in all subpopulations of $CAR^+$ cells, although their percentages varied (Figure 2B). Notably, more than 50% of CD26 $CAR^+$ cells expressed CD26, excluding the $CD4^+HIST^+$ T and $MT^+$ effector T cell subpopulations. Similarly, most $CAR^+$ subpopulations had more $CD44^+$ cells, except for $MT^+$ effector T and $CD4^+HLA^+$ naive T cells. However, the cellular

**Figure 1. Study design and clustering analysis of CAR-T scRNA-seq data**

(A) Fold change in the proliferation of nontransfected (NT) cells or CD44v6 CAR-T cells after 14 days of transduction compared with day 0. (B) Apoptosis of NT cells or CD44v6 CAR-T cells after 7 and 14 days of transduction. (C) Quantification of cytokines IFN-γ, TNF-α, IL-6, and IL-4 in the supernatant of NT or CD44v6 CAR-T cells after 14 days transfection via BD cytometric bead array. (D) Schematic of the study design for scRNA-seq and scTCR-seq. Peripheral blood mononuclear cells (PBMCs) were collected from two healthy donors, and T cells were sorted by $CD3^+$ staining. A CAR of CD19, CD26, or CD44v6 was constructed; after 14 days scRNA-seq combined with scTCR-seq was performed using the 10× Genomics platform. (E) Bar charts show the fraction of cells (left) and number of cells (right) in each sample among cell subpopulations. (F) Dot plot showing scaled expression levels of typical marker genes for each cell subpopulation colored by average expression. Dot size represents the percentage of cells in each cell subpopulation with more than one read of the corresponding gene. (G) UMAP plot of pooled $CAR^+$ T cells collected from all conditions of six samples. Each point represents a single cell, colored according to cell subpopulation. Statistical significance: $^*p < 0.05$, $^{***}p < 0.001$.

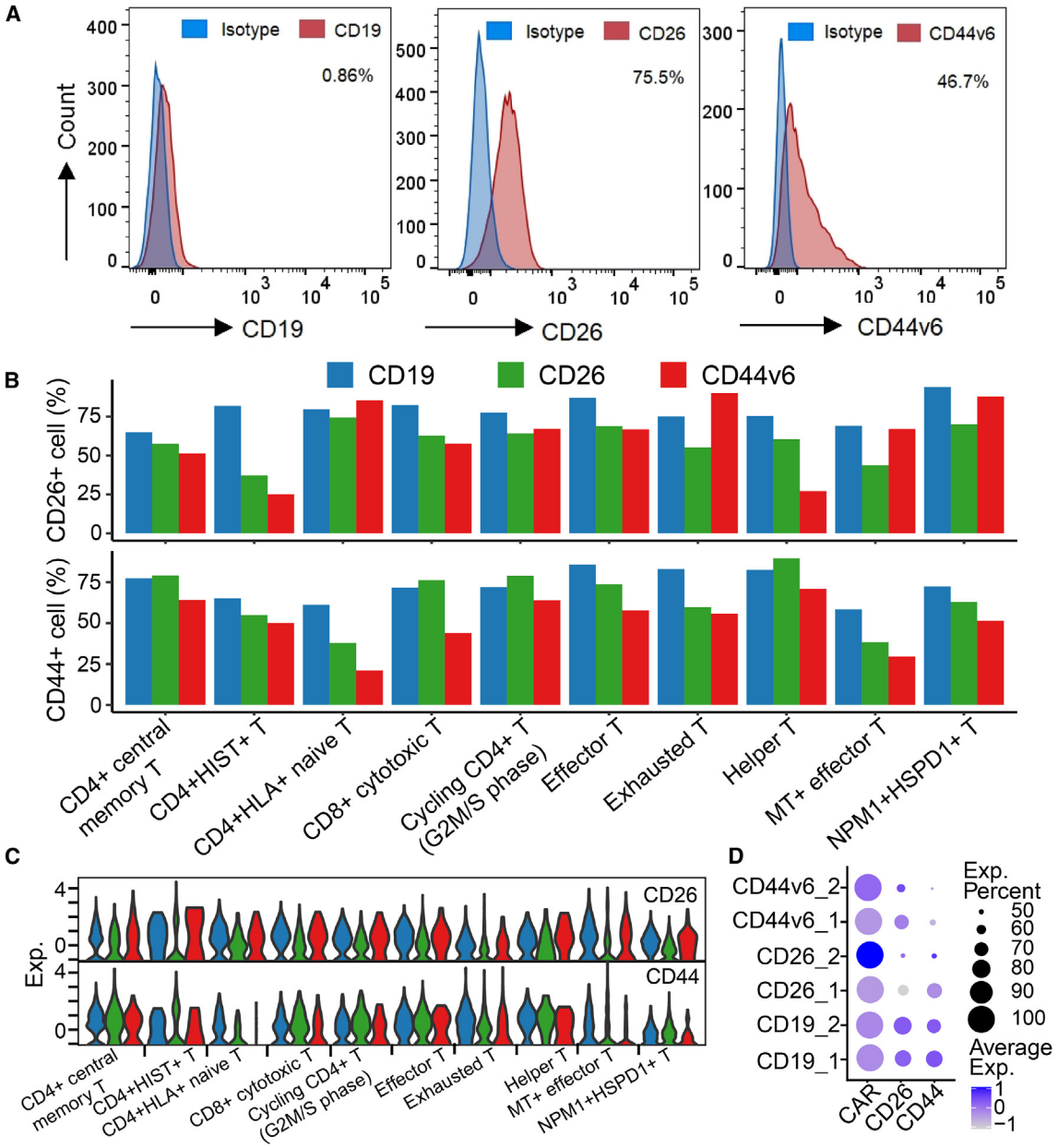


**Figure 2. The expression of the CAR-T target genes CD26 and CD44v6 in all cell subpopulations**

(A) The percentages of CD19-expressing ($CD19^+$) cells (left), CD26-expressing ($CD26^+$) cells (middle), and CD44v6-expressing ($CD44v6^+$) cells (right) in untransfected T cells were analyzed by flow cytometry. (B) Percentage of $CD26^+$ cells (top) and CD44-expressing ($CD44^+$) cells (bottom) in all $CAR^+$ cell subpopulations from single-cell sequencing data. (C) Log-normalized expression of the CD26 and CD44 genes for 10 T cell subpopulations. (D) Dot plot for the expression of the CD26, CD44, and CAR genes in $CAR^+$ cells of two donor samples.

content of fratricidal CAR-Ts expressing their target genes was commonly lower than that of CD19 CAR-Ts (Figure 2B). This was consistent with markedly lower CD26 or CD44 expression in CD26 CAR-T or CD44v6 CAR-T samples than in the other two CAR-Ts (Figures 2C and 2D). This suggests that, although the suicide effect exists, the survival of fratricidal CAR-Ts is accompanied by target gene expression.

### CD26 and CD44v6 CAR-T cells showed no unique T cell subpopulations but more clonal expansion of TCRs

Given that the survival of fratricidal CAR-Ts is not due to the target gene, is the survival dependent on specific cell subpopulations? In fact, all three CAR-T types contained all cell subpopulations, indicating no different types in the T cell subpopulations between CD19 CAR-Ts and fratricidal CAR-Ts (Figures 3A and S3A). All

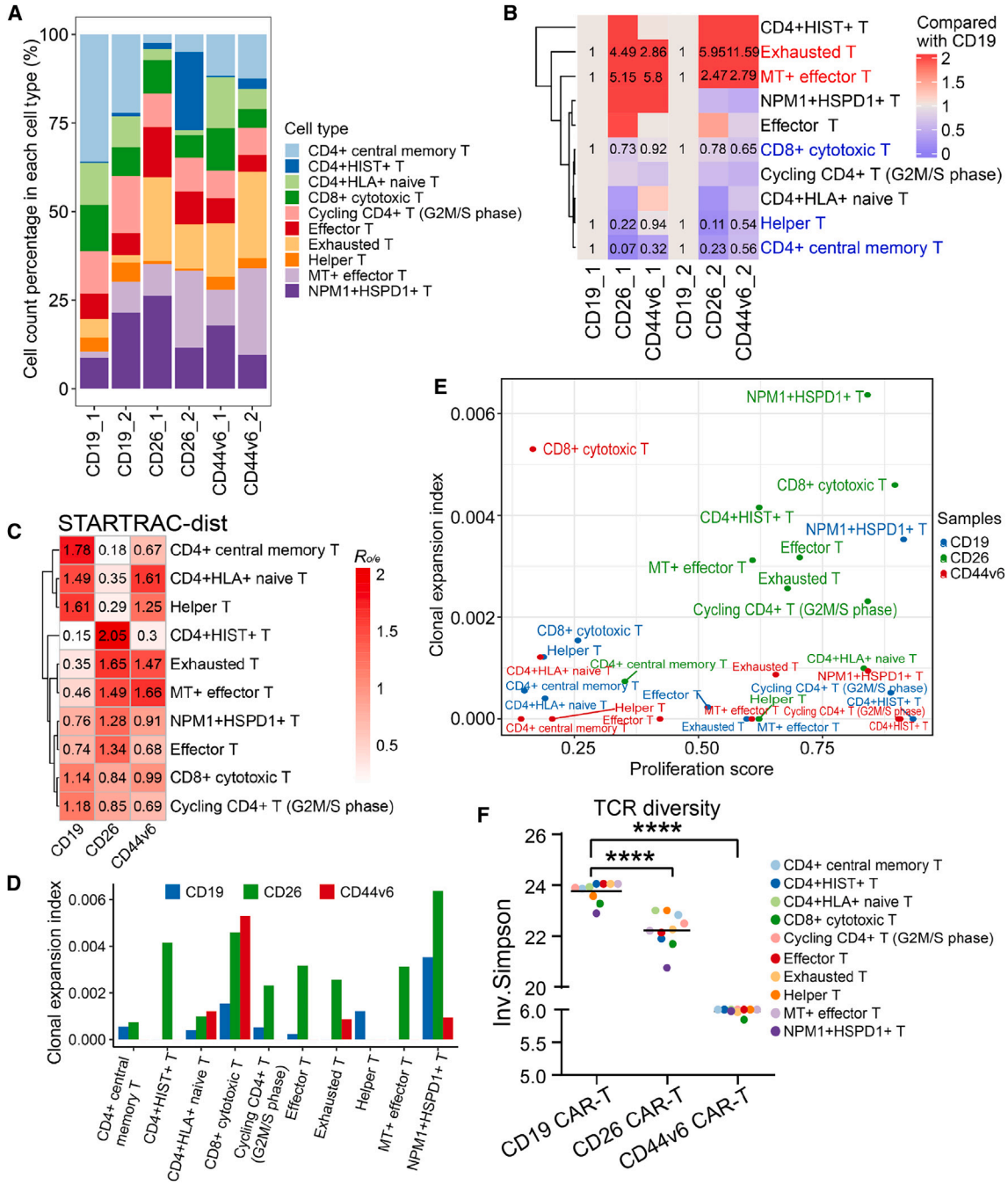


**Figure 3. Key subpopulations and their clonal expansion analyses of CAR$^+$ cells in CD26 and CD44v6 CAR-T**

(A) Bar charts show the percentage of each cell subpopulation among all CAR-expressing (CAR$^+$) cells in each sample. (B) Relative contents of all CAR$^+$ cell subpopulations (compared with CD19 CAR-T sample of the same individual) in all samples. Red font represents increased cell content in fratricidal CAR-T cells, and blue represents decreased. (C) Heatmap shows the CAR-T sample preference of various cell subpopulations with detected TCRs estimated by the STARTRAC-dist index of STARTRAC (see materials and methods), in which $R_{o/e}$ is the ratio of observed cell number over the expected cell number of a given combination of T cell subpopulation and sample. (D) Clonal expansion levels of different T cells quantified by STARTRAC-expa for each CAR-T cell subpopulation. (E) Distribution of proliferation score (x axis) vs. the clonal expansion index (y axis, STARTRAC-expa index). (F) TCR diversity of each cell subpopulation (Inv.Simpson index) among the three CAR-T types. Two-tailed paired t test; ****$p < 0.0001$.

three CAR-T types showed high percentages of NPM1$^+$HSPD1$^+$ T cells (Figure 3A). However, fratricidal CAR-Ts demonstrated higher proportions of exhausted T cells and fewer CD4$^+$ central memory T cells compared with CD19 CAR-Ts (Figures 3A and S1F; Table S3). In addition, CD26 CAR-T samples had the lowest ratio of helper T cells and naive T cells (Figure 3A). Consistent with the CAR$^+$ cells, fratricidal CAR-Ts contained more exhausted T cells and fewer cytotoxic T cells than CD19 CAR-Ts in CAR$^-$ cells (Figure S3A).

To explore key cell subpopulations of fratricidal CAR-Ts, the relative abundance of cell subpopulations against CD19 CAR-Ts for each donor was calculated (Figure 3B). The results showed that fratricidal CAR-Ts had lower percentages of CD4$^+$ central memory T, helper T, and CD8$^+$ cytotoxic T cells. Conversely, exhausted T and MT$^+$ effector T subpopulations were significantly higher than in CD19 CAR-Ts (Figures 3A and 3B).

Next, scTCR-seq coupled with previous scRNA-seq data analyzed the clone information within T cells across three CAR-T types. Notably, over 75% of cells had matched TCR information in CD19 CAR-Ts, which was higher than that in fratricidal CAR-Ts, while CD4$^+$HIST$^+$ T and MT$^+$ effector T cells had fewer clones than other subpopulations (Figures S4B and S4C). Compared with the CD19 CAR-Ts, the TCRs of exhausted T and MT$^+$ effector T cells were significantly enriched in fratricidal CAR-Ts (Figure 3C). In contrast, TCRs from CD4$^+$ central memory T and CD8$^+$ cytotoxic T cells were enriched in CD19 CAR-Ts compared with fratricidal CAR-Ts, which was consistent with the scRNA-seq profiles (Figures 3A and 3C). In addition, clonal expansion was evident in fratricidal CAR-T cell samples, especially in CD26 CAR-Ts (Figure 3D), which had more polyclonal cells in multiple cell subpopulations (Figure 3D). The correlation between proliferation levels and clonal expansion revealed that the highest proportion of amplified cells occurred in CD8$^+$ cytotoxic T and NPM1$^+$HSPD1$^+$ T cells of CD26 CAR-Ts (Figure 3E). In addition, fratricidal CAR-Ts exhibited significantly lower TCR diversity (y axis, inverse Simpson [Inv.Simpson] index) than CD19 CAR-Ts (Figure 3F). CD8$^+$ cytotoxic T and NPM1$^+$HSPD1$^+$ T cells had relatively low diversity, consistent with the amplification results (Figures 3E and 3F). Furthermore, the top 20 amplified TCR clonotypes in each CAR-T type were biased toward exclusivity (Figure S4D). These results suggest that fratricidal CAR-Ts have higher clonal expansion and lower diversity than CD19 CAR-Ts.

### T cell subpopulations prevalently show more exhaustion characteristics in CD26 and CD44v6 CAR-T

Functional status analyses demonstrated that the cytotoxicity and exhaustion of fratricidal CAR-Ts were higher in the absence of separating cell subpopulations, compared with control CD19 CAR-Ts without target stimulation (Figure 4A). Exhausted T cells had the highest levels of cytotoxicity and exhaustion (Figures 4B and 4C), which were consistent with the expression levels of cytotoxicity- and exhaustion-related genes (Figures S5A and S5B). Fratricidal CAR-Ts showed dramatically higher exhaustion than CD19 CAR-Ts in all cell subpopulations (Figure 4C) and significantly higher cytotoxicity levels over CD19 CAR-Ts in CD4$^+$ central memory T, CD8$^+$ cytotoxic T, and exhausted T cells. Further, flow cytometry revealed significantly high expression of the exhaustion markers LAG3 and HAVCR2 (Tim3) in fratricidal CAR-Ts (Figure 4D). The data also illustrated a significantly lower ($p \leq 0.05$) CD69 expression (T cell activation marker) in fratricidal CAR-Ts compared with CD19 CAR-Ts in most of the cell subpopulations (Figures 4A and 4E). Consistently, the proportion of CD69$^+$ cells in fratricidal CAR-Ts was less than in CD19 CAR-Ts (Figure 4F). These findings suggest that fratricidal CAR-Ts have lower activation and higher exhaustion status, which are associated with higher cytotoxicity levels.

### Fratricidal CAR-T cells may downregulate HLA molecules to escape immunity

To elucidate the molecular mechanism behind the survival of fratricidal CAR-Ts, we examined differential expression between fratricidal CAR-Ts and CD19 CAR-Ts for the five key cell subpopulations with abundance differences mentioned in Figure 3B. Results demonstrated that numerous cytokines were differentially expressed genes (DEGs) in five cell subpopulations, with CD26 CAR-Ts exhibiting elevated levels (Figure 5A). This is consistent with the previous analysis, where CD26 CAR-Ts had the highest cytotoxicity scores (Figure 4B).

Memory T cells are essential for the sustainability of CAR-T immunotherapy. Our data showed that 62 DEGs were simultaneously upregulated and 64 DEGs were simultaneously downregulated for CD26 CAR-Ts vs. CD19 CAR-Ts and CD44v6 CAR-Ts vs. CD19 CAR-Ts in CD4$^+$ central memory T cells (Figure 5B). Remarkably, the immunosuppressive genes LAG3 and HAVCR2 were upregulated in fratricidal CAR-Ts, while the immune activators CD27, TNFRSF14, and TNFSF138 were downregulated (Figure 5B). Interestingly, major histocompatibility complex (MHC) class I and II genes (e.g., HLA-DQA1, DPA1, etc.) were dramatically downregulated in fratricidal CAR-Ts in CD4$^+$ central memory T cells (Figure 5C). These downregulated DEGs were significantly enriched in inflammation-related pathways, antigen processing and presentation of peptide antigen via MHC II, and TCR-related pathways (Figures 5D and S6A). Moreover, HLA molecules were also poorly expressed in fratricidal CAR-Ts in helper T cells (Figure S6B). Previous research demonstrated that genomic loss of mismatched HLA in leukemia evades donor T cell recognition.[22] These results implied that fratricidal CAR-T cell subpopulations, including CD4$^+$ central memory T and helper T cells, may downregulate HLA molecules to evade elimination by conventional T cells and improve their survival.

### Regulation of key transcription factors drives the survival of fratricidal CAR-T cells

As mentioned above, fratricidal CAR-T cells display more exhaustion characteristics (Figure 4), and exhausted T cells are the most abundant cell subpopulations in fratricidal CAR-Ts (Figure 3A). We further analyzed their molecular profiles and regulation. The cytokines IL-22 and CSF2 and the chemokine CCL3 were decreased in

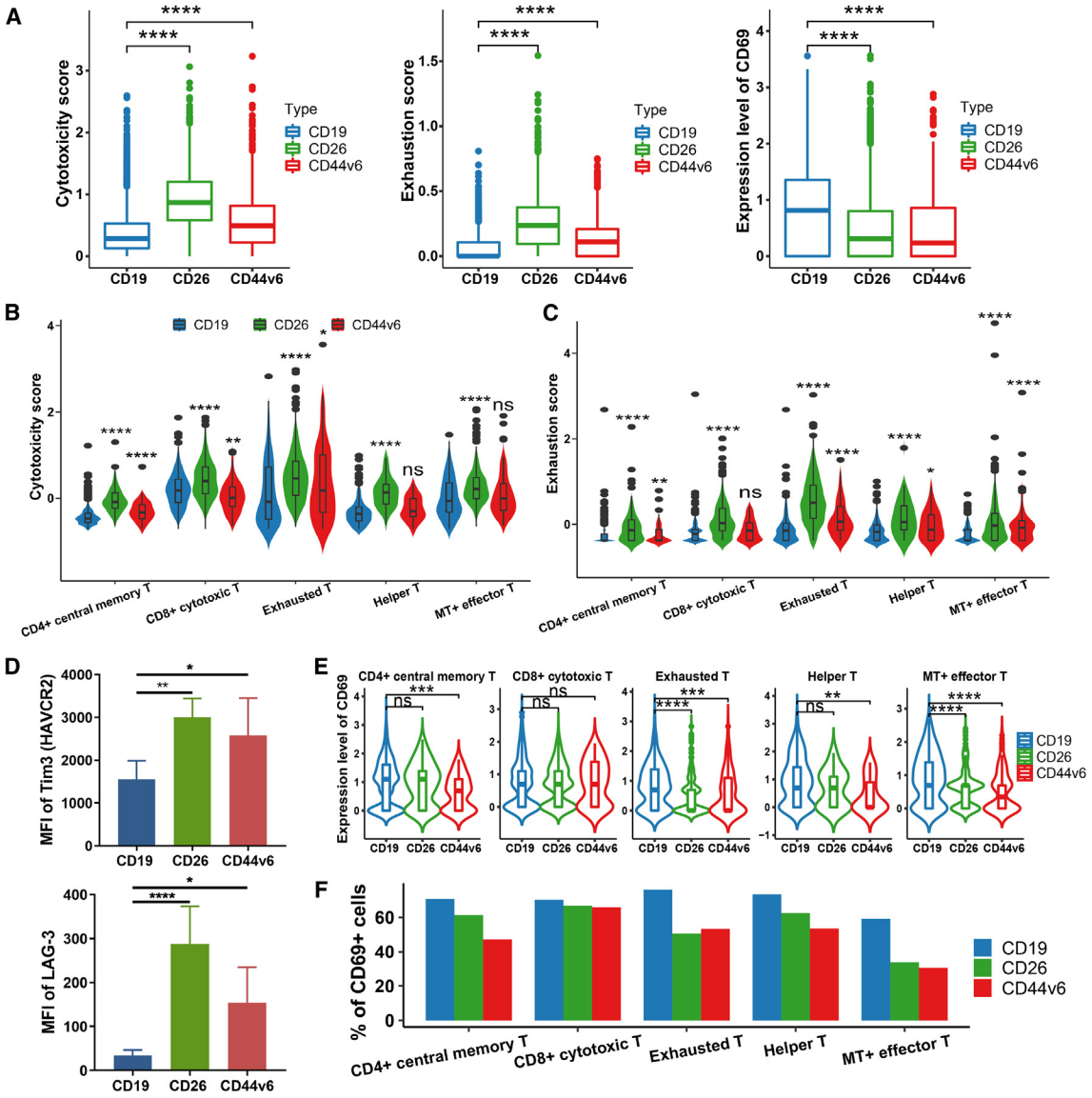


**Figure 4. Functional status analyses of different CAR-T types**

(A) Boxplots of cytotoxicity score, exhaustion score, and CD69 expression level of all CAR$^+$ cells in the three CAR-T types. Wilcoxon tests were used for all pairwise and group comparisons unless otherwise stated. (B and C) Violin plots of cytotoxicity score (B) and exhaustion score (C) for key subpopulations as mentioned in Figure 3B in the three CAR-T types. (D) Mean fluorescence intensity (MFI) of the T cell exhaustion markers LAG3 and Tim3 molecules. One-way analysis of variance (ANOVA), followed by Dunnett's *post hoc* test for multiple comparisons. (E and F) CD69 gene expression (E) and percentage of CD69$^+$ cells (F) in key subpopulations. Statistical significance: $^*p < 0.05$, $^{**}p < 0.01$, $^{***}p < 0.001$, $^{****}p < 0.0001$; ns indicates nonsignificance.

both CD26 and CD44v6 CAR-T cells in exhausted T cells, while the exhaustion-related genes LAG3 and IL-3 were significantly upregulated (Figure 6A). The DEGs were significantly enriched in cytokine-cytokine receptor interaction, hematopoietic cell lineage, JAK-STAT signaling pathway, and inflammation-related signaling pathways (Figure 6B). Furthermore, Gene Ontology (GO) biological process (BP) enrichment suggested involvement in T cell activation and regulation, negative regulation of immune system processes, lymphocyte-mediated immunity, etc. (Figure 6C). This implied that there would be more regulation of T cell signaling and the immune system in fratricidal CAR-T cells.

Next, to explore overrepresented regulons (transcription factors [TFs] and their target genes) in exhausted T cell subpopulations, we applied the single-cell regulatory network inference and clustering (SCENIC) method to score the activity of regulons (Figure 6D). Forty potential

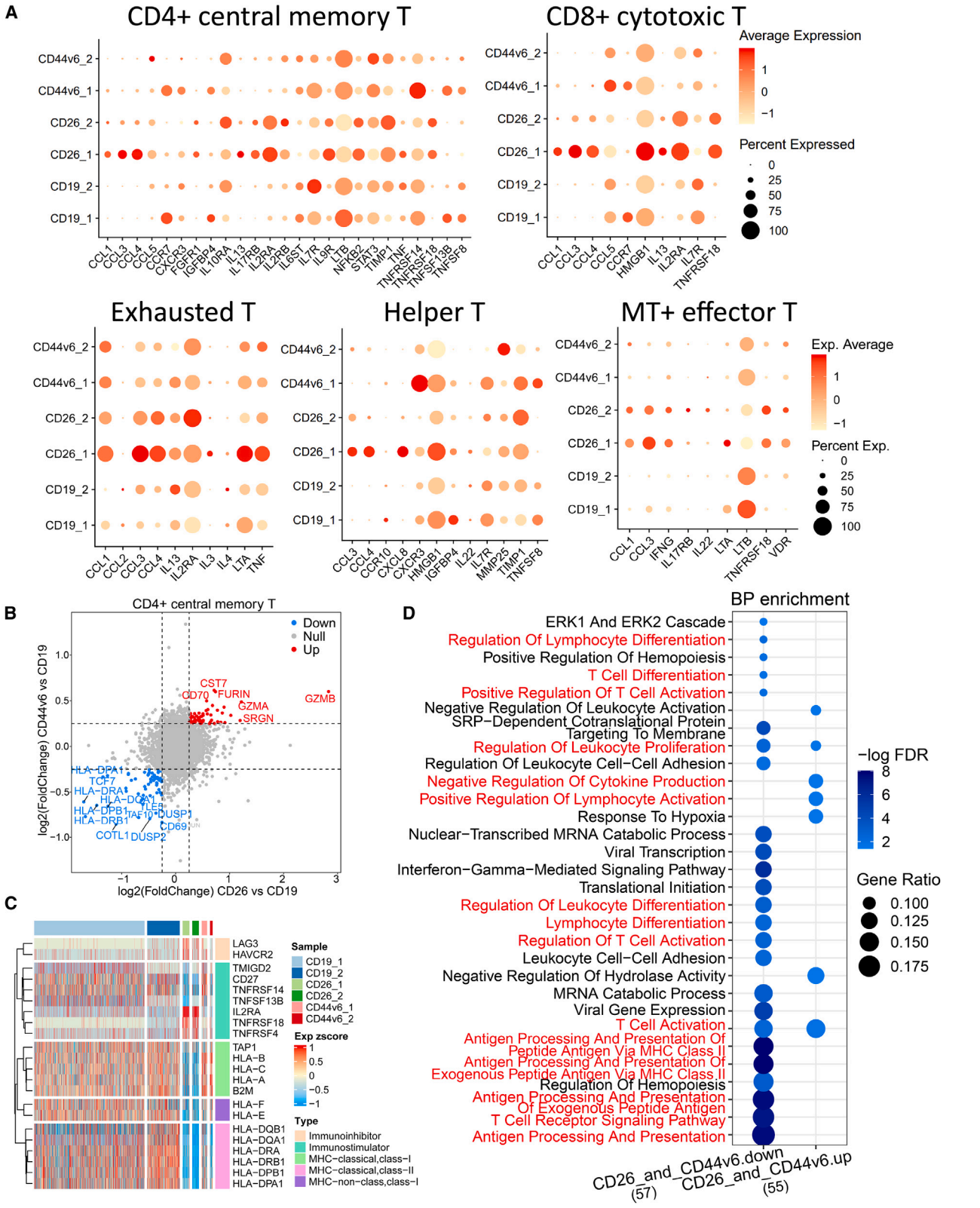


*(legend on next page)*

master regulons (including 28 TFs) were identified (Figures 6D and 6E), of which 16 (11 TFs) and 24 (17 TFs) were specifically enriched in CD19 CAR-T cells and fratricidal CAR-T cells, respectively (Figure S6C). For instance, RUNX3, YBX1, ATF4, and TBX21 regulons were highly expressed and active in fratricidal CAR-Ts, whereas STAT1, IRF1, and BATF3 regulons were downregulated in fratricidal CAR-T cells (Figures 6E and S6C). The regulatory network of exhausted T cells indicated that STAT1 and IRF1 act as core regulatory factors regulating genes involved in exhaustion, immune escape, and immune activation (Figure 6F). STAT1, IRF1, and BATF3 regulate numerous downregulated immune-escape genes (HLA-DRA, HLA-DQB1, HLA-DQA1, TAP1, etc.) and immunostimulatory factors (CD28, CD48, CD40LG, KLRK1, CXCR4, etc.) in exhausted T cell subpopulations (Figures 6F and S6D). Consistently, STAT1 and IRF1 have also been reported to be associated with T cell exhaustion.[23,24] ETS1 was significantly upregulated in fratricidal CAR-T cells, linked to the exhaustion factor T-bet,[25] and involved in regulating T cell exhaustion in pregnancy.[26] These results imply that a complex regulation of these critical TFs and target genes may contribute to the formation and survival of exhausted T cells in fratricidal CAR-T cells.

To validate the key regulatory roles of STAT1 and IRF1 in fratricidal CAR-T cells, we regulated the expression of STAT1 to assess its effect on fratricidal CAR-T functionality. Studies showed that IFN-γ can significantly upregulate STAT1 expression, and 2-NP can enhance the effect of IFN-γ on STAT1.[27] Therefore, CD44v6 CAR-T cells were pretreated with 45 μmol/L 2-NP for 1 h and then treated with 10 ng/mL IFN-γ for 72 h on the 10th day of construction. Subsequently, CD44v6 CAR-T function changes were observed (Figure S7A). The experimental results indicated that IFN-γ significantly upregulated the expression levels of STAT1 and IRF1 (Figure S7B) and decreased HLA-DPB1 expression (Figure S7C). In addition, while the expression of STAT1 and IRF1 was elevated, the expression levels of the exhaustion indicators Tim3 and LAG3 were downregulated (Figure S7D), and the specific cytotoxicity of CD44v6 CAR-Ts to tumor cells was also weakened (Figure S7E). Therefore, these data once again verified that the downregulation of the core regulatory factors STAT1 and IRF1 contributed to the survival and function of fratricidal CAR-T cells.

### Interfering with exhaustion marker genes may reduce the survival of fratricidal CAR-T cells

We conducted interference experiments to examine how T cell exhaustion influences the survival of fratricidal CAR-T cells. Studies have shown that ligand binding to inhibitory receptors on T cells, such as Tim3 and LAG3, mediates T cell exhaustion. Antibodies inhibiting these receptors can restore the function of exhausted T cells.[28,29] Two days after T cells were transfected with CD44v6 CAR lentivirus, cells were treated with the Tim3 inhibitor sabatolimab (an anti-Tim3 monoclonal antibody [mAb]) or the LAG3 inhibitor relatlimab (an anti-LAG3 mAb) at 10 and 20 μM for 7 and 14 days, respectively. Untreated CD44v6 CAR-T cells served as controls. Subsequently, the expression of Tim3 and LAG3 and the proliferation, apoptosis, and cytotoxicity of CD44v6 CAR-T cells were examined (Figure 7A). When CD44v6 CAR T cells were treated with inhibitors, the expression of exhaustion markers Tim3 and LAG3 decreased (Figure 7B), proliferation was inhibited (Figure 7C), apoptosis was increased (Figure 7D), and the specific cytotoxicity of CAR T cells to tumor cells was weakened (Figure 7E). This implies that arrest of the T cell exhaustion might reduce the survival of fratricidal CAR-T cells.

## DISCUSSION

CAR-T targeting of T cell malignancy will be fratricidal due to shared antigens on the surface of tumor cells and CAR-T cells. Nevertheless, previous studies have demonstrated that CAR-T cells targeting T cell malignancies, such as CD26 CAR-T and CD44v6 CAR-T cells, can be successfully obtained with good efficacy in prolonged culture time, despite initial fratricide.[17,19] However, the molecular mechanism of their survival is unclear. Is it due to target gene deletion or dependent on a specific T cell subpopulation? In this study, taking advantage of the single-cell transcriptome, we found significant differences in immune cell composition, clonal expansion, and gene expression between fratricidal CAR-T (CD26 and CD44v6 CAR-T) and CD19 CAR-T cells. The study provides preliminary insights into the characteristics and molecular mechanisms of fratricidal CAR-T cell survival.

Studies have reported that CAR-T cells may reduce fratricide by reducing target expression through an endocytic mechanism.[18,30] Our findings revealed that CD26 or CD44v6 was expressed in all cell subsets, although CD26 was least expressed in CD26 CAR-T cells and CD44v6 was least expressed in CD44v6 CAR-T cells. This implied that CD26 and CD44v6 CAR-T cells, although successfully expanded, still had fratricide. These findings suggested that the survival of fratricidal CAR-T cells did not depend on the deletion of target genes.

CAR-T expansion and efficacy may be affected by the functional heterogeneity of T cell subpopulations.[31] Using optimal T cell

**Figure 5. Differential expression analysis between fratricidal CAR-T cells and CD19 CAR-T cells**

(A) Dot plots of the expression levels of differentially expressed cytokine genes (cytokine DEGs) in $CD4^+$ central memory T cells, $CD8^+$ cytotoxic T cells, exhausted T cells, helper T cells, and $MT^+$ effector T cells of two donor samples. (B) Volcano plot of up- and downregulated genes in CD26 and CD44v6 CAR-T cells compared with CD19 CAR-T cells in $CD4^+$ central memory T cells. Genes with $|\log2(\text{FoldChange})| \geq 0.25$ in both comparison groups (CD26 vs. CD19 and CD44v6 vs. CD19) are highlighted. (C) Heatmap of differentially expressed immune-related genes, including immunoinhibitor, immunostimulator, and MHC molecules, in $CD4^+$ central memory T cells. Each column represents a cell, while each row indicates a gene. (D) Significantly (false discovery rate [FDR] $\leq 0.05$) enriched Gene Ontology biological process (BP) of consistently up- or downregulated genes from CD26 and CD44v6 CAR-T cells compared with CD19 CAR-T cells in $CD4^+$ central memory T cells. Dot color indicates the statistical significance of the enrichment (−log FDR), and dot size represents the gene ratio enriched in each term. Red terms, T cell and immune-related terms.

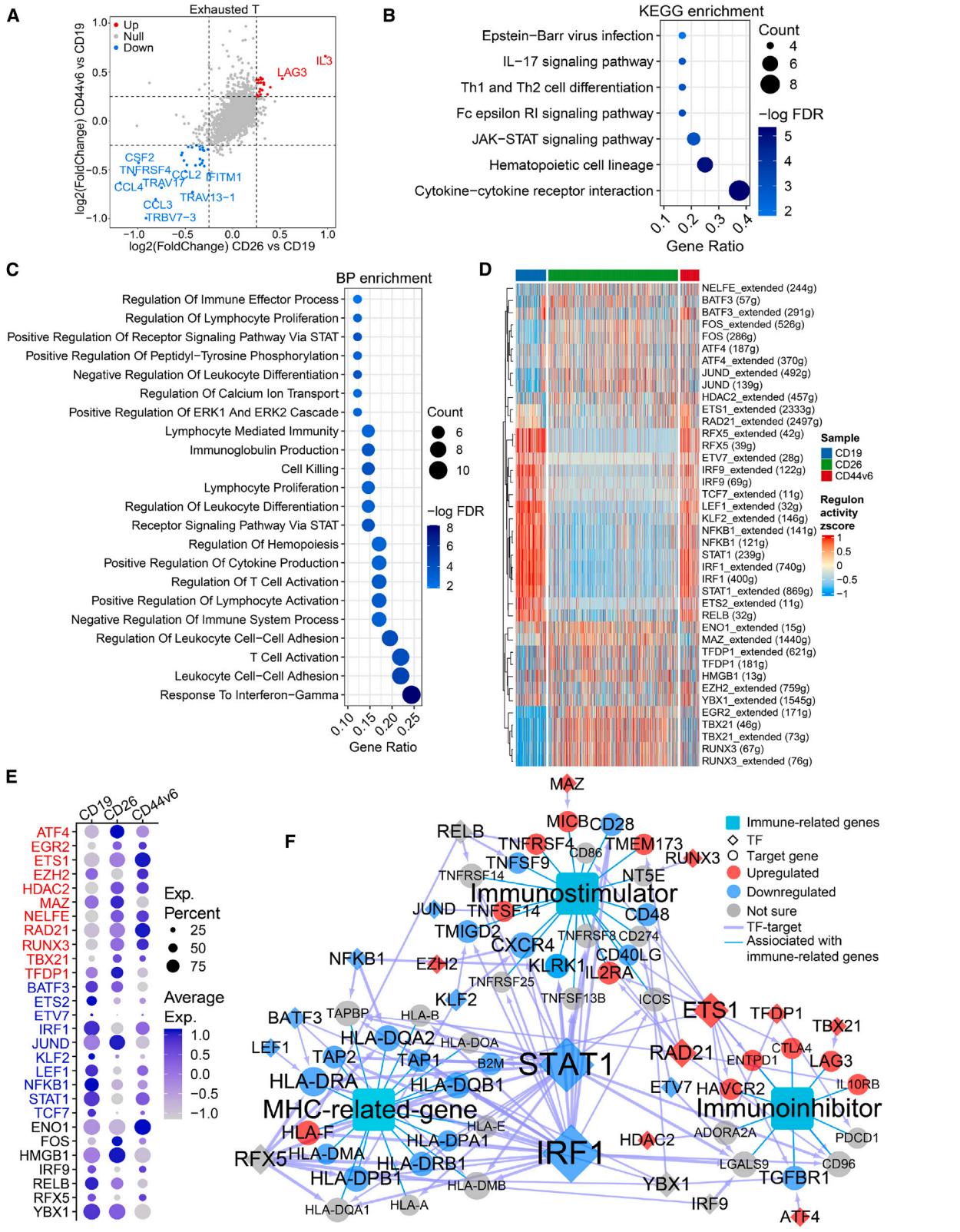


*(legend on next page)*

subpopulations may improve the design and manufacture of next-generation CAR-T cells with higher anticancer efficacy.[32] Logically, we wondered whether a specific subpopulation of T cells contributed to the survival of these CAR-Ts. Unfortunately, all CAR-T types shared the same subpopulations, and no subpopulation was unique to fratricidal CAR-T or CD19 CAR-T cells. Interestingly, among the three CAR-T cells, the cell subpopulation composition diverged; fratricidal CAR-Ts were enriched with higher contents of exhausted T and $MT^+$ effector T subpopulations, whereas CD19 CAR-Ts were enriched with higher contents of $CD4^+$ central memory T cells. It is hypothesized that it may be the presence of fratricide in fratricidal CAR-Ts that leads to the depletion of central memory T cells and the generation of effector Ts and exhausted Ts. Consequently, compared with CD19 CAR-Ts, fratricidal CAR-Ts did not have unique types in cell subpopulations.

Activation and exhaustion of CAR-Ts involve alterations in molecular expression and pathways.[33,34] To further explore the molecular mechanisms underlying the survival of fratricidal CAR-Ts, gene expression differences between fratricidal CAR-Ts and CD19 CAR-Ts were examined. It emerged that substantial HLA-class molecules (HLA-E, HLA-F, etc.) were downregulated in fratricidal CAR-T cells compared with CD19 CAR-T cells in a high proportion of cells (exhausted T cells) and low percentages of cell subpopulations (memory T cells and helper T cells). Multiple antigen presentation pathways associated with MHC molecules were downregulated in $CD4^+$ memory T cells of fratricidal CAR-Ts. Further, fratricidal CAR-T cells displayed fewer cellular communications and diminished communication strength among cell subpopulations compared with CD19 CAR-Ts (Figures S8A and S8B). Immune-escape-associated MHC-I and MHC-II pathway (HLA-related molecule ligand-receptor pairs) communication messages were consistently reduced in fratricidal CAR-T cells, and exhaustion-associated CD70 (CD70-CD27) signaling pathway communication messages were consistently elevated in fratricidal CAR-T cells (Figures S8C and S8D). This implied that cell-cell interactions could be a cause of cell exhaustion. Moreover, loss of HLA genes is a common mechanism by which target cells evade donor T cell recognition and leads to clinical relapse.[22,35,36] Consequently, we speculated that fratricidal CAR-T cell subpopulations may enhance immune escape by downregulating HLA genes to improve their survival.

In addition to downregulated HLA molecules, we hypothesized that the fratricidal CAR-T cell subpopulations might survive through exhaustion. Research indicates that long-term antigen stimulation induces T cell exhaustion.[33,37] Our data reinforced this conclusion with CD26 and CD44v6 CAR-T cells exhibiting more exhaustion characteristics, possibly due to target gene expression. Despite fratricidal CAR-Ts showing dramatically higher exhaustion levels than CD19 CAR-Ts in all cell subpopulations, $CD4^+$ central memory T, $CD8^+$ cytotoxic T, and exhausted T cells of fratricidal CAR-Ts showed significantly higher levels of cytotoxicity compared with CD19 CAR-T cells. In addition, clonal expansion was evident in fratricidal CAR-T cells. Therefore, we hypothesized that, in CD26 and CD44v6 CAR-T cells, the exhaustion induced by target antigen stimulation was in balance with the fratricide, so the presence of CAR-T cell exhaustion effectively prevented their fratricide. This hypothesis was further validated by the reduction in proliferation and the increase in apoptosis of CD44v6 CAR-T cells following inhibition of the exhaustion process by Tim3 or LAG3 inhibitors. This confirmed that the survival of fratricidal CAR-T cells may be dependent on their exhaustion.

In addition, the results of molecular mechanisms have reaffirmed that the survival of fratricidal CAR-T cells depends on cellular exhaustion. We found that exhaustion markers were highly expressed in terminally differentiated effector cells, such as exhausted T cells and $MT^+$ effector T cells, and then identified the regulation between key TFs and genes driving T cell exhaustion. For instance, STAT1 and IRF1 are linked to exhaustion,[23,24] acting as coregulators in a regulatory network and significantly downregulated in fratricidal CAR-T cells. These factors may regulate immune-escape genes (HLA genes) and immune-related factors, which is confirmed by the results of STAT1-overexpression experiments. Consistently, DEGs of fratricidal CAR-Ts in exhausted T cells were involved in the JAK-STAT pathway, which is involved in stem cell exhaustion during aging.[38] In addition, some potentially new exhaustion-associated TFs have been identified, such as ETS1, which upregulated many exhaustion marker genes (e.g., HAVCR2, ENTPD1, and LAG3), but further studies are needed. These results indicate that key factors might drive T cell exhaustion and thus the survival of fratricidal CAR-T cells.

This work is not without limitations. Although our findings initially indicate that the survival of fratricidal CAR-Ts may be related to

**Figure 6. Differential expression and regulatory analysis of exhausted T cells in three CAR-T types**

(A) Volcano plot of up- and downregulated genes in CD26 and CD44v6 CAR-T cells compared with CD19 CAR-T in exhausted T cells. Genes with $|\log2(\text{FoldChange})| \geq 0.25$ in both comparison groups (CD26 vs. CD19 and CD44v6 vs. CD19) are highlighted. (B and C) Significantly enriched (FDR $\leq$ 0.05) KEGG pathways (B) and GO biological processes (C) of DEGs from CD26 and CD44v6 CAR-Ts compared with CD19 CAR-Ts in exhausted T cells. Dot color indicates the statistical significance of the enrichment ($-\log$ FDR), and dot size represents the gene count enriched in each term. (D) Heatmap of the normalized regulon activity ($Z$ score, see materials and methods) derived from a generalized linear model of the difference between the three CAR-T types in exhausted T cells. Each column represents a cell, while each row indicates a regulon. A regulon name such as "RUNX3 (67g)" means a gene-regulatory network consisting of TF RUNX3 with its 67 high-confidence target genes. A regulon name such as "RUNX3_extended (76g)" indicates a gene-regulatory network consisting of TF RUNX3 with all 76 target genes. (E) Dot plot showing the scaled average expression of TFs in (D) for the three CAR-T-cell types. Red genes represent upregulation in fratricidal CAR-T cells, while blue genes represent downregulation. (F) Based on the regulons in (D), regulatory networks of key regulators on immune-related genes were constructed. The thickness of the edge represents the confidence score of the corresponding TF-regulated target gene.

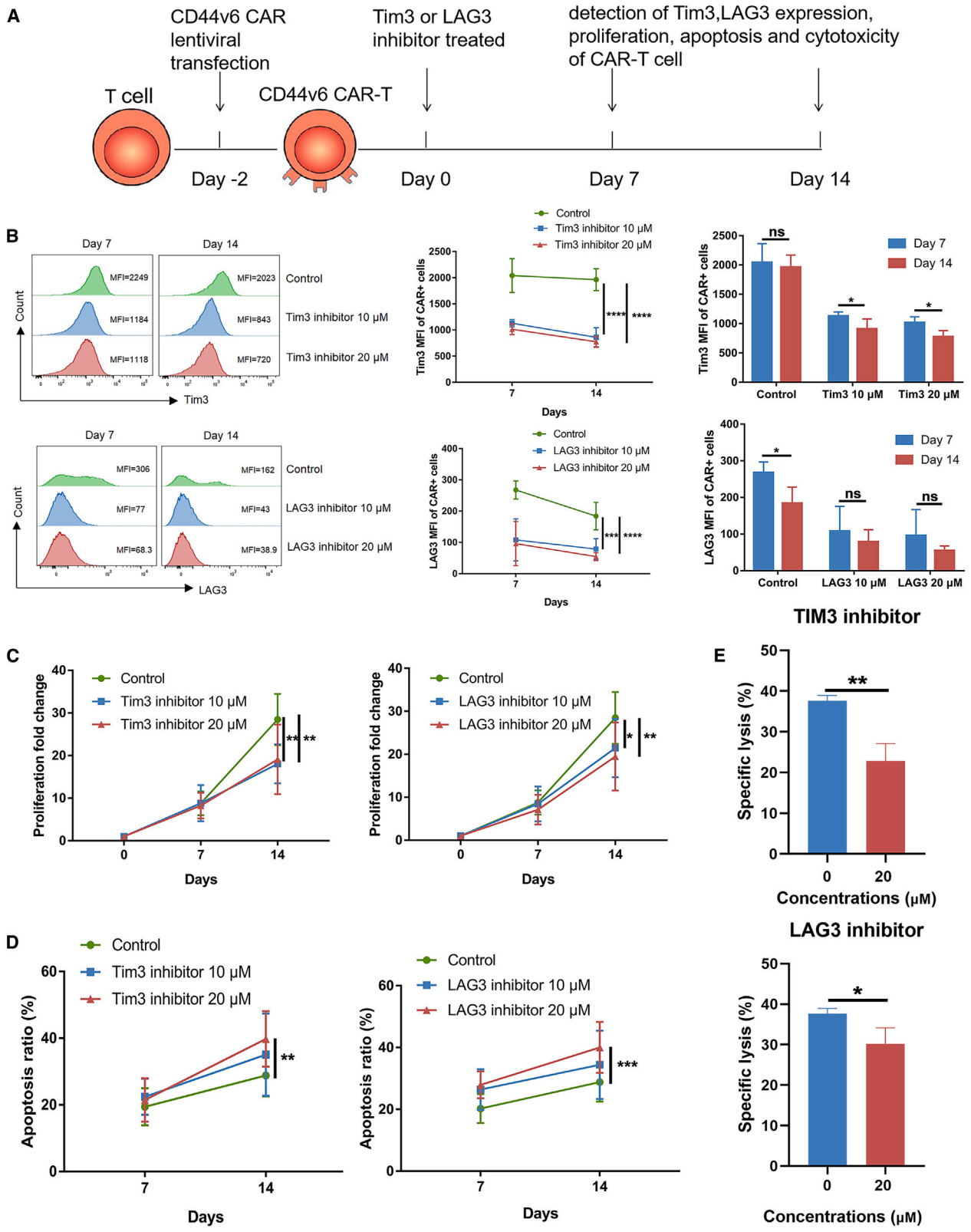


*(legend on next page)*

the downregulation of HLA molecules and the formation of exhausted T cells, additional comprehensive investigations are needed in the future to confirm our thesis. In particular, can consistent conclusions be drawn for protein-level expression? Moreover, the effect of interference with protein expression of key factors such as HLA molecules on the growth and proliferation of fratricidal CAR-Ts will be a further research direction. In addition, given that CD26 CAR-Ts contain a CD28 costimulatory structural domain, whereas CD19 CAR-Ts and CD44v6 CAR-Ts are 4-1BB (CD137) CAR-Ts, this may affect outcomes. However, Bai et al. revealed that the memory phenotype genes CCR7, SELL, and TCF7 were markedly upregulated in 4-1BB CAR-Ts vs. CD28 CAR-Ts in the basal state, with few other functional differences unique to the two CAR-T types.[39] This aligns with our transcriptional profiling results showing that CD26 CAR-Ts possessed a lower content of memory T cells than the remaining two CAR-Ts. Further, there is no unique cell subpopulation present in CD26 CAR-Ts in our data, and the convergent results for CD26 CAR-Ts and CD44v6 CAR-Ts could partially explain the survival of CAR-T products targeting T cell tumors.

In summary, our study reveals the heterogeneity of different CAR-T products. We found that CD26 and CD44v6 CAR-T cells targeting T cell malignancies were accompanied by the expression of target genes and had a higher exhaustion signature and clonal expansion status than CD19 CAR-T cells. They potentially downregulate HLA molecules to evade targeted killing by conventional T cells. Single-cell regulatory network analysis and inhibition experiments indicated that they may survive by driving their exhaustion through vital regulatory factors. The single-cell fratricidal CAR-T characteristics in this project will provide a theoretical basis for understanding the mechanisms of fratricidal CAR-T survival and help to guide the design of new and improved CAR production protocols targeting T cell malignancies.

## MATERIALS AND METHODS

### CAR-T cell production

After informed consent was obtained, T cells derived from two healthy donors were used to construct three types of CAR-Ts as mentioned above. All samples were obtained under the protocol approved by the Institutional Review Board of Tongji Medical College and the Hubei committee. CD19-CAR lentivirus containing anti-CD19-scFv-CD8-CD137-CD3ζ, CD26-CAR lentivirus containing anti-CD26-scFv-CD8-CD28-CD3ζ, and CD44v6-CAR lentivirus containing anti-CD44v6-scFv-CD8-CD137-CD3ζ were constructed by Shanghai GeneChem (China), and concentrated lentiviral stocks were frozen at −80°C for future use. $CD3^+$ T cells were isolated from the peripheral blood of healthy donors and cultured in X-VIVO15 (Lonza, USA) supplemented with 5% AB serum, 200 U/mL recombinant human IL-2 (PeproTech, USA), and 100 U/mL penicillin-streptomycin at 37°C in 5% $CO_2$. T cells were activated by CD3/CD28 beads (Miltenyi Biotech, Germany) according to the manufacturer's instructions. After 48 h, the activated T cells and CAR lentivirus were added to 96-well plates precoated with 6 μg/$cm^2$ Retronectin (Takara Bio, Japan), and the multiplicity of infection of CD19-CAR, CD26-CAR, and CD44v6-CAR lentivirus was 5, 10, and 3, respectively. Nontransfected cells (NT) were replaced with an equal volume of medium for virus. The mixtures were centrifuged at 800 × *g* for 30 min at 32°C and then incubated at 37°C for 24 h. The transfections were terminated by replacement of fresh X-VIVO15 medium. CD19, CD26, or CD44v6 CAR-T cells of two donors were cultured for 14 days and then subjected to scRNA-seq combined with scTCR-seq based on the 10× Genomics platform.

### scRNA-seq data processing

The scRNA-seq libraries were constructed using a Single Cell 5′ Library according to the manufacturer's instructions (10× Genomics). Libraries were sequenced using an Illumina Novaseq6000 sequencer with a paired-end 150-bp (PE150) reading strategy (performed by CapitalBio Technology). Raw gene expression matrices for each sample were obtained by Cell Ranger (v.4.0). The pipeline was coupled with the human reference version GRCh38. The output filtered gene expression matrices were analyzed by the R package Seurat (v.4.0.6).[40] Briefly, genes expressed at higher than 0.1% of the data and cells with >200 genes detected were retained for further analysis. Low-quality cells were removed if they met any of the following criteria: (1) <500 unique molecular identifiers (UMIs), (2) <500 or >7,500 genes, or (3) >15% of UMIs derived from the mitochondrial genome. Then, we used the DoubletFinder method[41] to detect doublets in each sample and remove them, finally resulting in high-quality cells for subsequent analysis. Multiple single-cell datasets were integrated and corrected for batch effects by the standard integration protocol described in Seurat. Gene expression matrices were normalized by the NormalizeData function, and 5,000 features with high cell-to-cell variation were calculated by the FindVariableFeatures function. To reduce the dimensionality of the datasets, the RunPCA function was performed with default parameters on linear-transformation-scaled data generated by the ScaleData function. Next, we clustered cells using the FindNeighbors and FindClusters functions and performed nonlinear dimensional reduction with the RunUMAP function set by default.

### Identification of $CAR^+$ T cells and estimation of abundance of expressed CAR

Based on previously published methods,[21] CAR-expressing T ($CAR^+$) cells were identified by the presence (normalized UMI > 0) of

**Figure 7. Function changes of CD44v6 CAR-T cells when the exhaustion was suppressed**

(A) Experimental design of CD44v6 CAR-T cells treated with the Tim3 inhibitor sabatolimab or LAG3 inhibitor relatlimab. (B) Tim3 (top) and LAG3 (bottom) expression levels in CD44v6 CAR-T cells treated with the Tim3 inhibitor sabatolimab or LAG3 inhibitor relatlimab at 10 and 20 μM for 7 and 14 days. Representative flow cytometry is shown on the left, and Tim3 or LAG3 expression analysis is shown on the middle and right. (C) Proliferation levels of CD44v6 CAR-T cells treated with Tim3 inhibitor (left) or LAG3 inhibitor (right). (D) Apoptosis of CD44v6 CAR-T cells treated with Tim3 inhibitor (left) or LAG3 inhibitor (right). (E) Specific cytotoxicity to tumor of CD44v6 CAR T cells treated with Tim3 and LAG3 inhibitors for 14 days. These experiments were repeated for five healthy donors. Data are depicted as the mean ± SD. Significance was determined by two-way ANOVA. $^*p < 0.05$, $^{**}p < 0.01$, $^{***}p < 0.001$, $^{****}p < 0.0001$; ns, not significant.

CAR-specific sequence contigs (signal peptide-CD19-scFv-CD8-CD137-CD3ζ, signal peptide-CD26-scFv-CD8-CD28-CD3ζ, and signal peptide-CD44v6-scFv-CD8-CD137-CD3ζ) in the aligned reads, and this approach identified a range of 2.11%–36.29% QC-passed T cells as $CAR^+$ cells among the three CAR-T types. Other T cells with undetectable CAR expression were defined as $CAR^-$ T cells. The expression level of CAR was estimated by the average depth of the CAR sequence in each sample. Sequencing reads were aligned to the reference CAR sequence, and reads with the best match flag (i.e., nonmismatch, nonmultiple hit, high quality) were kept to calculate the expressed CAR level. The expression level of CAR was normalized by the NormalizeData function by the Seurat package (v.4.0.0). Similarly, $CD26^+$ (CD26-expressing) cells and $CD44^+$ (CD44-expressing) cells were identified using the same method as above.

#### Flow cytometry analyses

For the expression of CD19, CD26, and CD44v6 markers on the surface of the T cells, T cells were incubated with CD19-BV421 (BD Biosciences, cat. no. 562441), CD26-PE (BD Biosciences, cat. no. 555437), and CD44v6-PE (BD Biosciences, cat. no. 566803) antibodies for 30 min at 4°C in the dark. For the apoptosis assessment, NT and CD44v6 CAR-T cells cultured in complete medium or CD44v6 CAR-T cells treated with the blocking anti-TIM3 mAb sabatolimab (Selleck, A2037) or anti-LAG3 mAb relatlimab (Selleck, A2029) were collected, and apoptotic cells were detected using an Annexin V-FITC/PI kit (BD Biosciences, cat. no. 556547). TIM3-PE (BD Biosciences, cat. no. 563422) and LAG3-Alexa 647 (BD Biosciences, cat. no. 565417) antibodies were used to assess the expression of TIM3 and LAG3 markers on the surface of the CAR-T cells. The cytokines in the supernatant of NT or CD44v6 CAR-T cells after 14 days of transfection were analyzed using the BD cytometric bead array (CBA). The samples were all detected by BD LSRFortessa X-20 flow cytometry and analyzed by FlowJo software.

#### Cell proliferation

The expansion of NT and CD44v6 CAR-T cells at different days of culture was assessed by trypan blue staining and counting under a microscope. CD44v6 CAR-T cells were treated with the Tim3 inhibitor sabatolimab and the LAG3 inhibitor relatlimab at concentrations of 10 and 20 μM, respectively. CD44v6 CAR-T cells were seeded at $2.5 \times 10^6$/mL density. Fresh medium with inhibitors was changed every 2 days for treatment times of 7 and 14 days. After 7 and 14 days, CD44v6 CAR-T cells were harvested, stained with trypan blue, and counted under a microscope. The proliferation fold change is the ratio of cell counts at different time points compared with cell counts at day 0.

#### STAT1 regulation in CD44v6 CAR-T cells

CD44v6 CAR-T cells were pretreated with 45 μmol/L 2-NP (MedChemExpress, HY-W013523) for 1 h and then treated with 10 ng/mL recombinant human IFN-γ (PeproTech, cat. no. 10773-476) for 72 h on the 10th day of construction. Subsequently, the expression of STAT1, IRF1, and HLA-DPB1 mRNA in CD44v6 CAR-T cells was detected by RT-qPCR, and the primer pairs used were as follows:

GAPDH: 5′-GGAGCCAAACGGGTCATCATCTC-3′ and 5′-GAGGGGCCATCCACAGTCTTCT-3′

STAT1: 5′-CAGCTTGACTCAAAATTCCTGGA-3′ and 5′-TGAAGATTACGCTTGCTTTTCCT-3′

IRF1: 5′-GCAGCTACACAGTTCCAGG-3′ and 5′-GTCCTCAGGTAATTTCCCTTCCT-3′

HLA-DPB1: 5′-CCATGATGGTTCTGCAGGTT-3′ and 5′-TCCCTGGAAAAGGTAATTCTCTGG-3′

#### Cytotoxicity assay

Different effector cell:target cell (E:T) ratios of 0:1, 1:1, and10:1were used when coculturing CD44v6 CAR-T cells treated with or without TIM3 inhibitor, LAG3 inhibitor, or IFN-γ with target cells that had been stained with CFSE (BD Bioscience, USA) for 24 h. Propidium iodide (PI; BD Pharmingen, USA) was used to identify dead target cells. The samples were detected by BD LSRFortessa X-20 flow cytometry and analyzed by FlowJo software. The cytotoxicity was assessed by the percentage of dead cells in target cells.

#### Cell-cycle regression

To remove variance (and unwanted effects on clustering) in the datasets arising from cell-cycle phase, we performed the CellCycleScoring function in Seurat to evaluate the cell-cycle status using the previously reported G1/S and G2/M phase-specific genes.[42] Cell-cycle effects were removed using the ScaleData function in Seurat.

#### Defining cell state scores

We calculated and defined the scores of cytotoxicity, exhaustion, proliferation, and apoptosis levels of cell subpopulations based on the expression of relevant molecules. The exhaustion score of T cells was defined as the mean of the *Z* score values of the expression of exhaustion-related genes (*CTLA4*, *LAG3*, *PDCD1*, *CD160*, *ENTPD1*, *HAVCR2*, and *TIGIT*).[43] The expression of each gene was normalized to the expression data by the SCTransform function of the Seurat package. We calculated the cytotoxicity, proliferation, and apoptosis scores based on cytotoxicity genes (*PRF1*, *IFNG*, *GNLY*, *NKG7*, *GZMB*, *GZMA*, *KLRK1*, *KLRD1*, *CTSW*, and *CST7*),[43] cell-cycle genes,[42] and apoptosis genes (*ACIN1*, *BIRC3*, *CYCS*, *NFKB1*, *PARP1*, *BCL2A1*, and *CDK1*),[39] respectively.

#### DEG identification and KEGG enrichment

Differential gene expression analysis was performed using the FindMarkers function based on normalized data in the Seurat R package. The samples we compared were entered as ident.1 and ident.2, respectively. The fold change in the mean gene expression level between the selected samples was calculated. For each comparison group (CD19 vs. CD26, CD19 vs. CD44v6, and CD26 vs. CD44v6) for each donor, genes that met the following threshold conditions were defined as DEGs: $|\text{avg\_log2FC}| \geq 0.25$, $p \leq 0.05$, and the

gene was expressed in >10% of cells. After that, the intersection of two donor DEGs with the same trend was used as the final DEG. Functional enrichment analyses, including GO BP and KEGG, were conducted using the compareCluster function from the clusterprofiler R package (v.4.0.5) (fun = "enrichKEGG", pvalueCutoff = 0.05, pAdjustMethod = "BH", OrgDb = "org.Hs.e.g.db").

#### Differential activity analysis of SCENIC regulons

To identify regulons controlling gene expression in different CAR-T types in exhausted T cells, we performed SCENIC analysis on the datasets of exhausted T cells (1,142 cells) of three CAR-T types using the cisTarget v.9 motif collection mc9nr (hg38) by R package SCENIC v.1.2.4.[44] The activity of regulons of exhausted T cells was calculated using the AUCell function with default parameters using a raw count matrix and was scaled by $Z$ score. Regulon specificity scores were ranked following the SCENIC pipeline, and top regulons with $Z$ scores higher than 1.7 were identified as the CAR-T-type regulon. The regulatory network was constructed based on the detected regulons and immune-related genes.

#### TCR V(D)J sequencing and analysis

For scTCR-seq, full-length TCR V(D)J segments were enriched from amplified cDNA from 5′ libraries via PCR amplification using a Chromium Single-Cell V(D)J Enrichment Kit according to the manufacturer's protocol (10× Genomics). Demultiplexing, gene quantification, and TCR clonotype assignment were performed using the Cell Ranger (v.4.0) vdj pipeline with GRCh38 as a reference. In brief, we obtained a TCR diversity metric containing clonotype frequency and barcode information. TCR analyses of $CAR^+$ cells were performed using the R package scRepertoire.[45] Only cells with at least one productive TCR α-chain (TRA) and one productive TCR β-chain (TRB) were kept for further analysis. Each unique TRA(s)-TRB(s) pair was defined as a clonotype. If one clonotype was present in at least two cells, then the cells harboring this clonotype were considered to be clonal, and the number of cells with such pairs indicated the degree of clonality of the clonotype. Using barcode information, T cells with prevalent TCR clonotypes were projected on UMAP plots. scTCR-seq data were merged with scRNA-seq data of the T cell subpopulations based on the cell barcode information. T cell dynamics across three CAR-T cell types were analyzed by the STARTRAC analysis toolkit.[46] STARTRAC-dist depicts the CAR-T-type distribution preference of different T cell subpopulations. The ratio of the cell number observed in the tissue to the expected number of cells was used to measure the enrichment of T cell populations in different tissues. The clonal expansion of T cells was calculated using STARTRAC-expa of STARTRAC.

#### Inferring cell-cell interactions using CellChat

To infer cell-cell communication between cell types identified in scRNA-seq analysis, we used the R package CellChat (v.1.6.1)[47] with default parameters. First, we converted the initial Seurat object to a CellChat object. Then, the CellChat receptor and ligand pair database was applied to the new object. We then performed an overrepresentation analysis of the genes and possible interactions in the CellChat database. The $p$-value threshold for significant ligand-receptor interactions was set to less than 0.05.

#### Statistical analysis

Unless specified, data are given as the mean ± SEM, were analyzed by GraphPad Prism 8, and are denoted in the figure legends. Violin plots in this paper were visualized by the R package ggplot2, using the Wilcoxon test for group comparisons. Unless otherwise stated, $p$ values below 0.05 were considered significant. Single, double, triple, and quadruple asterisks indicate statistical significance: $^*p < 0.05$, $^{**}p < 0.01$, $^{***}p < 0.001$, and $^{****}p < 0.0001$; ns indicates a nonsignificant result. If adjustments for multiple comparisons were needed, they were performed using the Holm-Bonferroni method, with adjusted $p < 0.05$ considered significant.

#### Data availability

The data generated in this study are available within the article and its supplemental information files. The scRNA-seq and scTCR-seq data are available at the Genome Sequence Archive (GSA) of the National Genomics Data Center (NGDC) under accession no. HRA002417 and can be accessed at URL: https://ngdc.cncb.ac.cn/.

## SUPPLEMENTAL INFORMATION

Supplemental information can be found online at https://doi.org/10.1016/j.omtn.2024.102225.

## ACKNOWLEDGMENTS

After informed consent was obtained, peripheral blood from healthy donors was collected under the protocol approved by the institutional review board of Tongji Medical College and the Hubei committee (ChiCTR-OPN-16008526). This work was supported by the National Key R&D Program of China (2021YFF0703704), the Natural Science Foundation of Hubei Province of China (2020CFA070 and 2020CFB790), the National Natural Science Foundation of China (82270183, 32100527, and 82271599), the Excellent Young Science Foundation Project of Tongji Hospital (2020YQ0012), the Open Project of Hubei Key Laboratory (2023KFZZ016), and the 1.3.5 project for disciplines of excellence from West China Hospital of Sichuan University (ZYYC23007).

## AUTHOR CONTRIBUTIONS

X.Z., A.-Y.G., and Q.L. designed the studies and edited the manuscript; Y.Y., P.Z., X.Z., A.-Y.G., and Q.L. assisted with the study design; M.H., L.T., H.H., Y.Z., and J.C. performed the experiments and analyzed the data; A.-Y.G., Y.Z., H.H., and L.T. analyzed the scRNA-seq and scTCR-seq data and wrote the manuscript; H.H. and L.T. interpreted the results and prepared figures; and all authors reviewed the manuscript.

## DECLARATION OF INTERESTS

The authors declare no potential competing interests.

## REFERENCES


1. Eshhar, Z., Waks, T., Gross, G., and Schindler, D.G. (1993). Specific activation and targeting of cytotoxic lymphocytes through chimeric single chains consisting of antibody-binding domains and the gamma or zeta subunits of the immunoglobulin and T-cell receptors. Proc. Natl. Acad. Sci. USA *90*, 720–724. https://doi.org/10.1073/pnas.90.2.720.
2. Levine, B.L., Miskin, J., Wonnacott, K., and Keir, C. (2017). Global Manufacturing of CAR T Cell Therapy. Mol. Ther. Methods Clin. Dev. *4*, 92–101. https://doi.org/10.1016/j.omtm.2016.12.006.
3. Schuster, S.J., Svoboda, J., Chong, E.A., Nasta, S.D., Mato, A.R., Anak, Ö., Brogdon, J.L., Pruteanu-Malinici, I., Bhoj, V., Landsburg, D., et al. (2017). Chimeric Antigen Receptor T Cells in Refractory B-Cell Lymphomas. N. Engl. J. Med. *377*, 2545–2554. https://doi.org/10.1056/NEJMoa1708566.
4. Sadelain, M. (2017). CD19 CAR T Cells. Cell *171*, 1471. https://doi.org/10.1016/j.cell.2017.12.002.
5. Mullard, A. (2021). FDA approves first BCMA-targeted CAR-T cell therapy. Nat. Rev. Drug Discov. *20*, 332. https://doi.org/10.1038/d41573-021-00063-1.
6. Wagner, J., Wickman, E., DeRenzo, C., and Gottschalk, S. (2020). CAR T Cell Therapy for Solid Tumors: Bright Future or Dark Reality? Mol. Ther. *28*, 2320–2339. https://doi.org/10.1016/j.ymthe.2020.09.015.
7. Fleischer, L.C., Spencer, H.T., and Raikar, S.S. (2019). Targeting T cell malignancies using CAR-based immunotherapy: challenges and potential solutions. J. Hematol. Oncol. *12*, 141. https://doi.org/10.1186/s13045-019-0801-y.
8. Bayón-Calderón, F., Toribio, M.L., and González-García, S. (2020). Facts and Challenges in Immunotherapy for T-Cell Acute Lymphoblastic Leukemia. Int. J. Mol. Sci. *21*, 7685. https://doi.org/10.3390/ijms21207685.
9. Pan, J., Tan, Y., Wang, G., Deng, B., Ling, Z., Song, W., Seery, S., Zhang, Y., Peng, S., Xu, J., et al. (2021). Donor-Derived CD7 Chimeric Antigen Receptor T Cells for T-Cell Acute Lymphoblastic Leukemia: First-in-Human, Phase I Trial. J. Clin. Oncol. *39*, 3340–3351. https://doi.org/10.1200/JCO.21.00389.
10. Liu, J., Zhang, Y., Guo, R., Zhao, Y., Sun, R., Guo, S., Lu, W., and Zhao, M. (2023). Targeted CD7 CAR T-cells for treatment of T-Lymphocyte leukemia and lymphoma and acute myeloid leukemia: recent advances. Front. Immunol. *14*, 1170968. https://doi.org/10.3389/fimmu.2023.1170968.
11. Lu, P., Liu, Y., Yang, J., Zhang, X., Yang, X., Wang, H., Wang, L., Wang, Q., Jin, D., Li, J., and Huang, X. (2022). Naturally selected CD7 CAR-T therapy without genetic manipulations for T-ALL/LBL: first-in-human phase 1 clinical trial. Blood *140*, 321–334. https://doi.org/10.1182/blood.2021014498.
12. Zhao, Y. (2019). CD26 in autoimmune diseases: The other side of "moonlight protein.". Int. Immunopharm. *75*, 105757. https://doi.org/10.1016/j.intimp.2019.105757.
13. Enz, N., Vliegen, G., De Meester, I., and Jungraithmayr, W. (2019). CD26/DPP4 - a potential biomarker and target for cancer therapy. Pharmacol. Ther. *198*, 135–159. https://doi.org/10.1016/j.pharmthera.2019.02.015.
14. Heider, K.-H., Kuthan, H., Stehle, G., and Munzert, G. (2004). CD44v6: a target for antibody-based cancer therapy. Cancer Immunol. Immunother. *53*, 567–579. https://doi.org/10.1007/s00262-003-0494-4.
15. Grewal, I.S. (2008). CD70 as a therapeutic target in human malignancies. Expert Opin. Ther. Targets *12*, 341–351. https://doi.org/10.1517/14728222.12.3.341.
16. Jacobs, J., Deschoolmeester, V., Zwaenepoel, K., Rolfo, C., Silence, K., Rottey, S., Lardon, F., Smits, E., and Pauwels, P. (2015). CD70: An emerging target in cancer immunotherapy. Pharmacol. Ther. *155*, 1–10. https://doi.org/10.1016/j.pharmthera.2015.07.007.
17. Zhou, S., Li, W., Xiao, Y., Zhu, X., Zhong, Z., Li, Q., Cheng, F., Zou, P., You, Y., and Zhu, X. (2021). A novel chimeric antigen receptor redirecting T-cell specificity towards CD26+ cancer cells. Leukemia *35*, 119–129. https://doi.org/10.1038/s41375-020-0824-y.
18. Zhou, S., Zhu, X., Shen, N., Li, Q., Wang, N., You, Y., Zhong, Z., Cheng, F., Zou, P., and Zhu, X. (2019). T cells expressing CD26-specific chimeric antigen receptors exhibit extensive self-antigen-driven fratricide. Immunopharmacol. Immunotoxicol. *41*, 490–496. https://doi.org/10.1080/08923973.2019.1637889.
19. Tang, L., Huang, H., Tang, Y., Li, Q., Wang, J., Li, D., Zhong, Z., Zou, P., You, Y., Cao, Y., et al. (2022). CD44v6 chimeric antigen receptor T cell specificity towards AML with FLT3 or DNMT3A mutations. Clin. Transl. Med. *12*, e1043. https://doi.org/10.1002/ctm2.1043.
20. Wu, G., Guo, S., Luo, Q., Wang, X., Deng, W., Ouyang, G., Pu, J.J., Lei, W., and Qian, W. (2023). Preclinical evaluation of CD70-specific CAR T cells targeting acute myeloid leukemia. Front. Immunol. *14*, 1093750. https://doi.org/10.3389/fimmu.2023.1093750.
21. Deng, Q., Han, G., Puebla-Osorio, N., Ma, M.C.J., Strati, P., Chasen, B., Dai, E., Dang, M., Jain, N., Yang, H., et al. (2020). Characteristics of anti-CD19 CAR T cell infusion products associated with efficacy and toxicity in patients with large B cell lymphomas. Nat. Med. *26*, 1878–1887. https://doi.org/10.1038/s41591-020-1061-7.
22. Vago, L., Perna, S.K., Zanussi, M., Mazzi, B., Barlassina, C., Stanghellini, M.T.L., Perrelli, N.F., Cosentino, C., Torri, F., Angius, A., et al. (2009). Loss of mismatched HLA in leukemia after stem-cell transplantation. N. Engl. J. Med. *361*, 478–488. https://doi.org/10.1056/NEJMoa0811036.
23. Shao, Y.-J., Ni, J.-J., Wei, S.-Y., Weng, X.-P., Shen, M.-D., Jia, Y.-X., and Meng, L.-N. (2020). IRF1-mediated immune cell infiltration is associated with metastasis in colon adenocarcinoma. Medicine (Baltim.) *99*, e22170. https://doi.org/10.1097/MD.0000000000022170.
24. Ryan, N., Anderson, K., Volpedo, G., Hamza, O., Varikuti, S., Satoskar, A.R., and Oghumu, S. (2020). STAT1 inhibits T-cell exhaustion and myeloid derived suppressor cell accumulation to promote antitumor immune responses in head and neck squamous cell carcinoma. Int. J. Cancer *146*, 1717–1729. https://doi.org/10.1002/ijc.32781.
25. Grenningloh, R., Kang, B.Y., and Ho, I.-C. (2005). Ets-1, a functional cofactor of T-bet, is essential for Th1 inflammatory responses. J. Exp. Med. *201*, 615–626. https://doi.org/10.1084/jem.20041330.
26. Lewis, E.L., Xu, R., Beltra, J.-C., Ngiow, S.F., Cohen, J., Telange, R., Crane, A., Sawinski, D., Wherry, E.J., and Porrett, P.M. (2022). NFAT-dependent and -independent exhaustion circuits program maternal CD8 T cell hypofunction in pregnancy. J. Exp. Med. *219*, e20201599. https://doi.org/10.1084/jem.20201599.
27. Lynch, R.A., Etchin, J., Battle, T.E., and Frank, D.A. (2007). A small-molecule enhancer of signal transducer and activator of transcription 1 transcriptional activity accentuates the antiproliferative effects of IFN-gamma in human cancer cells. Cancer Res. *67*, 1254–1261. https://doi.org/10.1158/0008-5472.CAN-06-2439.
28. Zhao, L., Cheng, S., Fan, L., Zhang, B., and Xu, S. (2021). TIM-3: An update on immunotherapy. Int. Immunopharm. *99*, 107933. https://doi.org/10.1016/j.intimp.2021.107933.
29. Zhou, G., Sprengers, D., Boor, P.P.C., Doukas, M., Schutz, H., Mancham, S., Pedroza-Gonzalez, A., Polak, W.G., de Jonge, J., Gaspersz, M., et al. (2017). Antibodies Against Immune Checkpoint Molecules Restore Functions of Tumor-Infiltrating T Cells in Hepatocellular Carcinomas. Gastroenterology *153*, 1107–1119.e10. https://doi.org/10.1053/j.gastro.2017.06.017.
30. Mamonkin, M., Rouce, R.H., Tashiro, H., and Brenner, M.K. (2015). A T-cell–directed chimeric antigen receptor for the selective treatment of T-cell malignancies. Blood *126*, 983–992. https://doi.org/10.1182/blood-2015-02-629527.
31. Golubovskaya, V., and Wu, L. (2016). Different Subsets of T Cells, Memory, Effector Functions, and CAR-T Immunotherapy. Cancers *8*, 36. https://doi.org/10.3390/cancers8030036.
32. Brudno, J.N., and Kochenderfer, J.N. (2018). Chimeric antigen receptor T-cell therapies for lymphoma. Nat. Rev. Clin. Oncol. *15*, 31–46. https://doi.org/10.1038/nrclinonc.2017.128.
33. Zhu, X., Hu, H., Xiao, Y., Li, Q., Zhong, Z., Yang, J., Zou, P., Cao, Y., Meng, F., Li, W., et al. (2022). Tumor-derived extracellular vesicles induce invalid cytokine release and exhaustion of CD19 CAR-T Cells. Cancer Lett. *536*, 215668. https://doi.org/10.1016/j.canlet.2022.215668.
34. Zhang, Q., Hu, H., Chen, S.-Y., Liu, C.-J., Hu, F.-F., Yu, J., Wu, Y., and Guo, A.-Y. (2019). Transcriptome and Regulatory Network Analyses of CD19-CAR-T Immunotherapy for B-ALL. Dev. Reprod. Biol. *17*, 190–200. https://doi.org/10.1016/j.gpb.2018.12.008.
35. Waterhouse, M., Pfeifer, D., Pantic, M., Emmerich, F., Bertz, H., and Finke, J. (2011). Genome-wide profiling in AML patients relapsing after allogeneic hematopoietic cell transplantation. Biol. Blood Marrow Transplant. *17*, 1450–1459.e1. https://doi.org/10.1016/j.bbmt.2011.07.012.

36. Crucitti, L., Crocchiolo, R., Toffalori, C., Mazzi, B., Greco, R., Signori, A., Sizzano, F., Chiesa, L., Zino, E., Lupo Stanghellini, M.T., et al. (2015). Incidence, risk factors and clinical outcome of leukemia relapses with loss of the mismatched HLA after partially incompatible hematopoietic stem cell transplantation. Leukemia *29*, 1143–1152. https://doi.org/10.1038/leu.2014.314.

37. Tang, L., Kong, Y., Wang, H., Zou, P., Sun, T., Liu, Y., Zhang, J., Jin, N., Mao, H., Zhu, X., et al. (2023). Demethylating therapy increases cytotoxicity of CD44v6 CAR-T cells against acute myeloid leukemia. Front. Immunol. *14*, 1145441. https://doi.org/10.3389/fimmu.2023.1145441.

38. Li, X., Zeng, X., Xu, Y., Wang, B., Zhao, Y., Lai, X., Qian, P., and Huang, H. (2020). Mechanisms and rejuvenation strategies for aged hematopoietic stem cells. J. Hematol. Oncol. *13*, 31. https://doi.org/10.1186/s13045-020-00864-8.

39. Bai, Z., Lundh, S., Kim, D., Woodhouse, S., Barrett, D.M., Myers, R.M., Grupp, S.A., Maus, M.V., June, C.H., Camara, P.G., et al. (2021). Single-cell multiomics dissection of basal and antigen-specific activation states of CD19-targeted CAR T cells. J. Immunother. Cancer *9*, e002328. https://doi.org/10.1136/jitc-2020-002328.

40. Butler, A., Hoffman, P., Smibert, P., Papalexi, E., and Satija, R. (2018). Integrating single-cell transcriptomic data across different conditions, technologies, and species. Nat. Biotechnol. *36*, 411–420. https://doi.org/10.1038/nbt.4096.

41. McGinnis, C.S., Murrow, L.M., and Gartner, Z.J. (2019). DoubletFinder: Doublet Detection in Single-Cell RNA Sequencing Data Using Artificial Nearest Neighbors. Cell Syst. *8*, 329–337.e4. https://doi.org/10.1016/j.cels.2019.03.003.

42. Tirosh, I., Izar, B., Prakadan, S.M., Wadsworth, M.H., Treacy, D., Trombetta, J.J., Rotem, A., Rodman, C., Lian, C., Murphy, G., et al. (2016). Dissecting the multicellular ecosystem of metastatic melanoma by single-cell RNA-seq. Science *352*, 189–196. https://doi.org/10.1126/science.aad0501.

43. Guo, X., Zhang, Y., Zheng, L., Zheng, C., Song, J., Zhang, Q., Kang, B., Liu, Z., Jin, L., Xing, R., et al. (2018). Global characterization of T cells in non-small-cell lung cancer by single-cell sequencing. Nat. Med. *24*, 978–985. https://doi.org/10.1038/s41591-018-0045-3.

44. Van de Sande, B., Flerin, C., Davie, K., De Waegeneer, M., Hulselmans, G., Aibar, S., Seurinck, R., Saelens, W., Cannoodt, R., Rouchon, Q., et al. (2020). A scalable SCENIC workflow for single-cell gene regulatory network analysis. Nat. Protoc. *15*, 2247–2276. https://doi.org/10.1038/s41596-020-0336-2.

45. Borcherding, N., Bormann, N.L., and Kraus, G. (2020). scRepertoire: An R-based toolkit for single-cell immune receptor analysis. F1000Res. *9*, 47. https://doi.org/10.12688/f1000research.22139.2.

46. Zhang, L., Yu, X., Zheng, L., Zhang, Y., Li, Y., Fang, Q., Gao, R., Kang, B., Zhang, Q., Huang, J.Y., et al. (2018). Lineage tracking reveals dynamic relationships of T cells in colorectal cancer. Nature *564*, 268–272. https://doi.org/10.1038/s41586-018-0694-x.

47. Jin, S., Guerrero-Juarez, C.F., Zhang, L., Chang, I., Ramos, R., Kuan, C.-H., Myung, P., Plikus, M.V., and Nie, Q. (2021). Inference and analysis of cell-cell communication using CellChat. Nat. Commun. *12*, 1088. https://doi.org/10.1038/s41467-021-21246-9.